

# Electronic Properties and Applications of Single-Walled Carbon Nanotubes

Nan Zheng

*Course: Solid State II*

*Instructor: Elbio Dagotto*

*Spring 2008*

*Department of Physics*

*University of Tennessee*

*Email: [nzheng@utk.edu](mailto:nzheng@utk.edu)*

# Electronic Properties and Applications of Single-Walled Carbon Nanotubes

## Abstract:

Carbon nanotubes have highly promising applications in future molecular electronics due to their unique electronic properties. This review begins with a brief introduction to experimental facts of structural and electronic properties of carbon nanotubes. The next section focuses on electronic structures of single walled carbon nanotube using the tight-binding model. Following that, applications of both semiconducting and metallic carbon nanotubes are presented. Finally the future developments of carbon nanotubes in both academic research industrial applications are discussed.

## 1. Introduction

Carbon nanotubes are hollow cylinders composed of pure carbon with diameters of a few nanometers and lengths of many microns. A single-walled carbon nanotube (SWNT) may be conceived as a graphene, which is a single atomic layer of graphite, rolled into a seamless cylinder, while Multi-walled carbon nanotubes (MWNT) consist of several layers of rolled graphite. Both SWNT and MWNT have similar mechanical and electronic properties. Because of the geometrical simplicity of the SWNT, this paper will mainly focus on SWNT. Using modern microscopes like TEM and AFM, detailed structures of carbon nanotubes can be observed in experiments (see Fig. 1).

The remarkable electronic properties of carbon nanotubes stem largely from the electronic structure of graphene, from which these nanotubes are derived. Graphene is a zero-gap semi-metal. While in most directions of the graphene sheet, energy gaps are not zero and electrons are not free to flow unless extra energy is provided, in certain special directions, energy gaps are zero and thus graphene displays the metallic property. In the band structure of graphene, conduction band and valence band contact each other at discrete points in  $k$ -space. However, when the graphene is rolled up into the nanotube, the direction along the axis of the nanotube is selected in the graphene sheet. Depending on geometric relation between the rolling direction and primitive vectors of the graphene sheet, the produced nanotube can be either metal or semiconductor. Since both metals and semiconductors can be made from the same all-carbon system, nanotubes are ideal candidates for molecular electronics technologies.

The nanotube axis direction relative to the graphene is denoted by a pair of integers  $(n, m)$  [1]. Depending on the appearance of a belt of carbon bonds along the peripheral of the nanotube cross section, the nanotube is classified into either an armchair ( $n = m$ ), or zigzag ( $n = 0$  or  $m = 0$ , but not both zero), or chiral (any other  $n$  and  $m$ ) structure. All armchair SWNTs are metals; those with  $n - m = 3k$ , where  $k$  is a nonzero integer, are semiconductors with a tiny band gap; and all others are semiconductors with a band gap that inversely depends on the nanotube diameter [1]. Figs. 1 (A),(B),(C) show the three different types of rolling-up pattern from a graphene sheet.

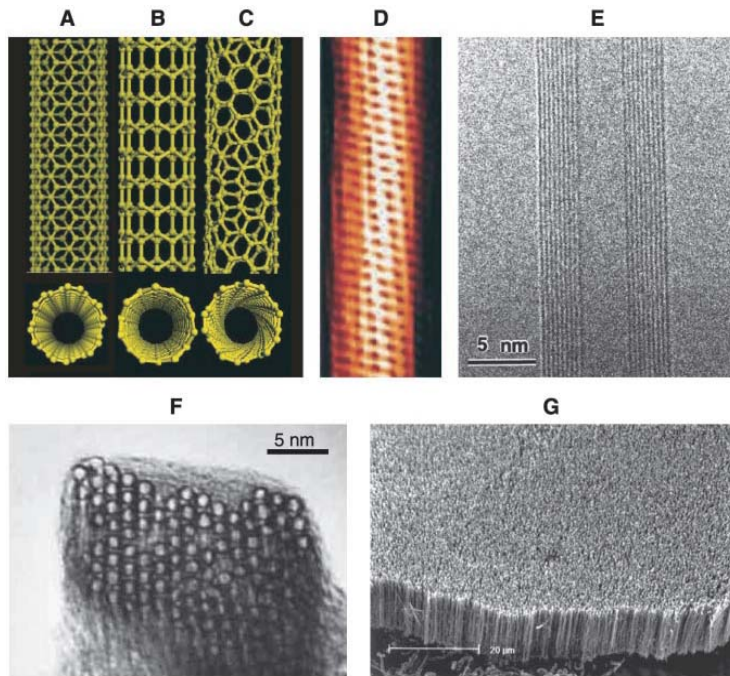


**Fig. 1:**

Schematic illustrations of the structures of (A) armchair, (B) zigzag, and (C) chiral SWNTs.

Projections normal to the tube axis and perspective views along the tube axis are on the top and bottom, respectively.

(D) Tunneling electron microscope image [2] showing the helical structure of a 1.3-nm-diameter chiral SWNT.

(E) Transmission electron microscope (TEM) image of a MWNT containing a concentric nested array of nine SWNTs.

(F) TEM micrograph [3] showing the lateral packing of 1.4-nm-diameter SWNTs in a bundle.

(G) Scanning electron microscope (SEM) image of an array of MWNTs grown as a nanotube forest. [4]

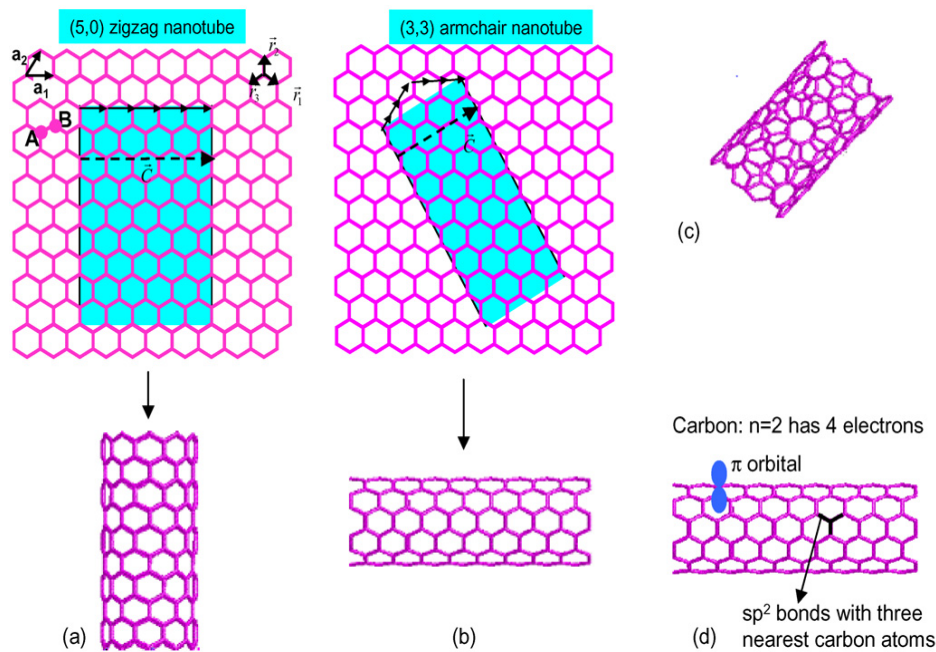


**Fig. 2:**

(a)  $a_1$  and  $a_2$  are the lattice vectors of graphene.  $|a_1| = |a_2| = \sqrt{3} a$ , where  $a$  is the carbon-carbon bond length. There are two atoms per unit cell shown by A and B. SWNTs are equivalent to cutting a strip in the graphene sheet (blue) and rolling them up such that each carbon atom is bonded to its three nearest neighbours. The creation of a  $(n, 0)$  zigzag nanotube is shown.

(b) Creation of a  $(n, n)$  armchair nanotube.

(c) A  $(n, m)$  chiral nanotube.

(d) The bonding structure of a nanotube. The  $n = 2$  quantum number of carbon has four electrons. Three of these electrons are bonded to its three nearest neighbours by  $sp^2$  bonding, in a manner similar to graphene. The fourth electron is a  $\pi$  orbital perpendicular to the cylindrical surface. [5]

## 2. Electronic structures of carbon nanotubes

Each carbon atom in the hexagonal lattice on a 2D graphene sheet possesses six valent electrons, among which are three  $2sp^2$  electrons and one  $2p$  electron. The three  $2sp^2$  electrons form the three bonds in the plane of the graphene sheet, leaving an unsaturated  $\pi$  orbital [5] (Fig. 2(d)). These  $\pi$  orbitals, perpendicular to the graphene sheet and thus the nanotube surface when the graphene sheet is rolled, form a delocalized network on the surface of the nanotube, responsible for its electronic properties.

First, it is beneficial to introduce the secular equation of tight-binding model, which is described below,

$$\hat{H}\vec{C}_i = E_i(\vec{k})\hat{S}\vec{C}_i, \quad (2.1)$$

where  $\hat{H}$  and  $\hat{S}$  are called transfer integral matrices and overlap integral matrices respectively, which are defined by

$$\begin{aligned} H_{jj'}(\vec{k}) &= \langle \Phi_j | \hat{H} | \Phi_{j'} \rangle, \\ S_{jj'}(\vec{k}) &= \langle \Phi_j | \Phi_{j'} \rangle \quad (j, j' = 1, \dots, n), \end{aligned} \quad (2.2)$$

here  $\Phi_j$  denotes the atom wavefunction of position  $j$  which is interested in.

A carbon atom at position  $\vec{r}_s$  has an unsaturated  $2p$  orbital described by the wave function  $\chi_{\vec{r}_s}(\vec{r})$ . In the nearest neighbour approach of tight-binding model, the interaction between orbitals on different atoms vanishes unless the atoms are nearest neighbours. Mathematically, this can be written as

$$\begin{aligned} \langle \chi_{\vec{r}_A} | H | \chi_{\vec{r}_A} \rangle &= \langle \chi_{\vec{r}_B} | H | \chi_{\vec{r}_B} \rangle = 0, \\ \langle \chi_{\vec{r}_A} | H | \chi_{\vec{r}_B} \rangle &= \langle \chi_{\vec{r}_B} | H | \chi_{\vec{r}_A} \rangle = \gamma \delta_{\vec{r}_A - \vec{r}_B = a}, \end{aligned} \quad (2.3)$$

here  $\gamma$  is the transfer integral constant.

To calculate the electronic structure, the Bloch wavefunction for each of the sublattices is constructed as

$$\phi_{s\vec{k}}(\vec{r}) = \sum_{\vec{r}_s} e^{i\vec{k}\cdot\vec{r}_s} \chi_{\vec{r}_s}(\vec{r}) = \gamma(e^{i\vec{k}\cdot\vec{R}_1} + e^{i\vec{k}\cdot\vec{R}_2} + e^{i\vec{k}\cdot\vec{R}_3}) \equiv \gamma f(k) \quad (2.4)$$

where  $s = A$  or  $B$  refers to each sublattice and  $\vec{r}_s$  refers to the set of points belonging to sublattice  $s$ ,  $\vec{R}_1$ ,  $\vec{R}_2$ ,  $\vec{R}_3$  are distance vector to the three nearest neighbors respectively.

Plug in those geometrical values and one can get,

$$f(\vec{k}) = e^{ik_x a / \sqrt{3}} + 2e^{-ik_x a / 2\sqrt{3}} \cos\left(\frac{k_y a}{2}\right), \quad (2.5)$$

Then the explicit forms for the transfer and overlap integral matrices---- $\hat{H}$  and  $\hat{S}$ ---- can be written as:

$$\hat{H} = \begin{pmatrix} \varepsilon_{2p} & \gamma f(k) \\ \gamma f(k)^* & \varepsilon_{2p} \end{pmatrix}, \quad \hat{S} = \begin{pmatrix} 1 & 0 \\ 0 & 1 \end{pmatrix}. \quad (2.6)$$

Note that  $\hat{S}$  is written as unity matrix due to the none-overlapping approximation which is

made before the calculation.

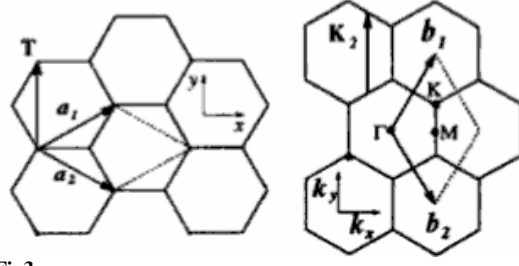


**Fig3:**  
Part of the unit cell and extended Brillouin zon of an armchair carbon nanotube.  $\vec{a}_i$  and  $\vec{b}_i$  are unit vectors and reciprocal lattice vectors of two-dimensional graphite, respectively. In the figure, the translational vector  $\vec{T}$  and the corresponding reciprocal lattice vector  $\vec{K}_2$ .

Solving the secular equation  $\det(\hat{H} - E\hat{S}) = 0$  and using  $\hat{H}$  and  $\hat{S}$  as given above, the eigen values  $E_k$  are obtained as a function of  $\vec{k}$  and  $w(\vec{k})$ :

$$E(\vec{k}) = \frac{\varepsilon_{2p}}{1 \pm \gamma w(\vec{k})},$$

$$\text{where } w(\vec{k}) = \sqrt{|f(\vec{k})|^2} = \sqrt{1 + 4 \cos \frac{\sqrt{3}k_x a}{2} \cos \frac{k_y a}{2} + 4 \cos^2 \frac{k_y a}{2}}. \quad (2.7)$$

If we use the parameter  $\varepsilon_{2p} = 0$ , the dispersion relation becomes

$$E_g(k_x, k_y) = \pm \gamma \left\{ 1 + 4 \cos \left( \frac{\sqrt{3}k_x a}{2} \right) \cos \left( \frac{k_y a}{2} \right) + 4 \cos^2 \left( \frac{k_y a}{2} \right) \right\}^{1/2}, \quad (2.8)$$

which is pictured in Fig. 3. In the picture, we can see the valence band and conduction band contact at six points at the corners of the Brillouin zone.

A more generalized calculation with an overlapping parameter  $t$  yields the following dispersion function:

$$E(\vec{k}) = \frac{\varepsilon_{2p} \pm t w(\vec{k})}{1 \pm \gamma w(\vec{k})} \quad \text{with } w(\vec{k}) = \sqrt{|f(\vec{k})|^2} = \sqrt{1 + 4 \cos \frac{\sqrt{3}k_x a}{2} \cos \frac{k_y a}{2} + 4 \cos^2 \frac{k_y a}{2}}. \quad (2.9)$$

Fig. 4 pictures this dispersion behavior using  $t = -3.033\text{eV}$  and  $\gamma = 0.129\text{eV}$  in order to reproduce the first principles calculation of the graphite energy bands[6].

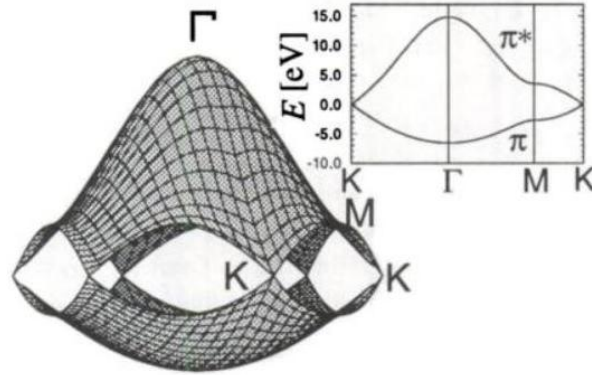


**Fig. 4:** The energy dispersion relation for 2D graphene with non-zero overlap are shown throughout the whole region of the Brillouin zone. The inset shows the energy dispersion along the high symmetry directions of the triangle  $\Gamma$ -M-K. [7]

To obtain the electronic structure of CNTs, we start from the band structure of graphene and quantize the wavevector in the circumferential direction. The simplest case to consider are the nanotubes having the highest symmetry, we mainly focus on an armchair nanotube (see Fig. 2 for definition of armchair structure). The appropriate periodic boundary condition used to obtain the energy eigenvalues is:

$$n\sqrt{3}k_{x,q}a = 2\pi q, \quad (q = 1, \dots, 2n).$$

(with  $n$  to be the chiral integer of armchair nanotubes) (2.10)

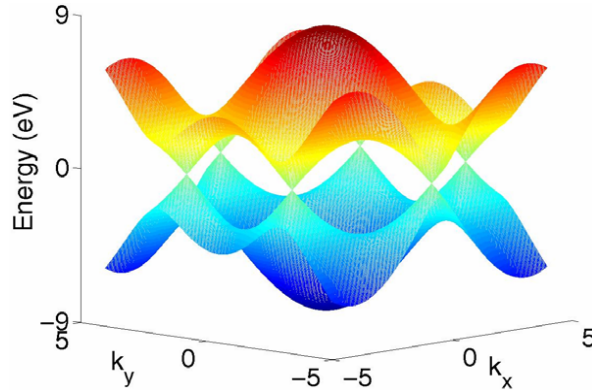


**Fig. 3:** electronic structure calculated within a non-overlapping tight-binding model. [5]

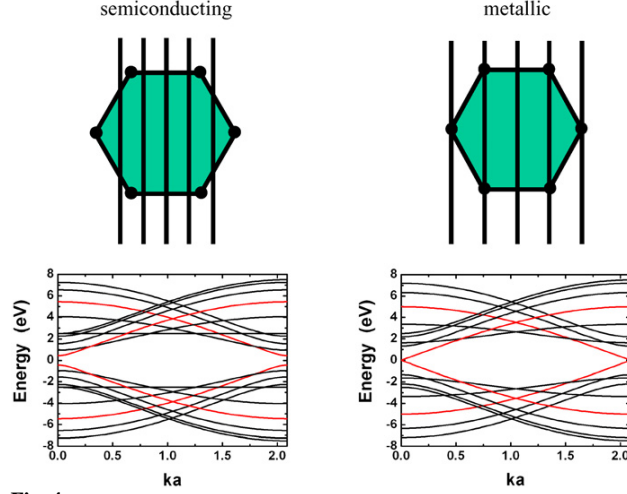


**Fig. 4:** Illustration of allowed wavevector lines leading to semiconducting and metallic CNTs and examples of bandstructures for semiconducting and metallic zigzag CNTs. [5]

Plug the above equation into Equation (2.9) gives the energy dispersion relation  $E_q^a(k)$  for the armchair nanotube,

$$E_q^a(k) = \pm \gamma \left\{ 1 \pm 4 \cos\left(\frac{q\pi}{n}\right) \cos\left(\frac{ka}{2}\right) + 4 \cos^2\left(\frac{ka}{2}\right) \right\}^{1/2},$$

$$(-\pi < ka < \pi), \quad (q = 1, \dots, 2n) \quad (2.11)$$

A more detailed analysis of the  $E(k)$  relations for chiral nanotubes is generally given by [8]

$$E(k) = \pm \gamma \left[ 1 + 4 \cos\left(\frac{3C_x ka}{2C} - \frac{3\pi a C_y}{C^2}\right) \cos\left(\frac{\sqrt{3}C_x ka}{2C} - \frac{\sqrt{3}\pi a C_y}{C^2}\right) + 4 \cos^2\left(\frac{\sqrt{3}C_y ka}{2C} + \frac{\sqrt{3}\pi a C_x}{C^2}\right) \right]$$

$$(2.12)$$

where  $k$  is the wavevector in the axial direction,  $C_x = a(\sqrt{3}n + (\sqrt{3}/2)m)$  and  $C_y = a(3/2)m$ .

Bandstructures for semiconducting and metallic CNTs calculated from this expression are shown in Fig. 4.

As discussed above, the condition for CNTs to be metallic is that some of the allowed lines cross one of the Fermi points of graphene. This leads to the condition where  $I$  is an integer. Nanotubes for which this condition does not hold are semiconducting. Furthermore, it can be shown that the bandgap of semiconducting nanotubes decreases with an increase in the diameter. The relationship between the bandgap and diameter [9, 10] can be obtained by finding the two lines that come closest to a graphene Fermi point, giving a bandgap,  $E_g \sim \gamma a / R$ , as shown in Fig. 4.

Finally, it is important to note that there are some deviations in the electronic properties of nanotubes from the simple-orbital graphene picture described above, due to curvature. As a

result of curvature, (i) the hopping integrals describing the three bonds between nearest neighbours are not identical and (ii) hybridization and charge self-consistency become important. Since curvature becomes larger with a decrease in the nanotube diameter, deviations from the simple orbital graphene picture become more distinct in small diameter nanotubes. Nanotubes satisfying  $n - m = 3l$  develop a small bandgap induced by the curvature and are hence semi-metallic. Armchair nanotubes are an exception because of their special symmetry, and they remain metallic for all diameters. The bandgap of semi-metallic nanotubes is small and varies inversely as the square of nanotube diameter. For example, while a semiconducting nanotube with a diameter of  $10\text{\AA}$  has a bandgap of  $1\text{ eV}$ , a semi-metallic nanotube with a comparable diameter has a bandgap of only  $40\text{ meV}$ . In graphene, hybridization between  $s$  and  $p$  orbitals is absent. In contrast, the curvature of a nanotube induces  $sp^2$  hybridization and the resulting in changes in long-range interactions. While the influence of hybridization in affecting the electronic properties of large diameter nanotubes is negligible, small diameter nanotubes are significantly affected. [9] found that while tight-binding calculations predict small diameter (4,0) and (5,0) zigzag nanotubes to be semiconducting with bandgaps exceeding  $1\text{ eV}$ , DFT-LDA calculations show that they are semi-metallic. Similarly, while tight-binding calculations predict the (6,0) zigzag nanotube to be semi-metallic with a bandgap of approximately  $200\text{ meV}$ , DFT-LDA calculations indicate that they are metallic [11,12]. Overall, small diameter nanotubes require a more careful treatment beyond the simple tight-binding graphene model.

### 3. Semiconducting CNTs as Field effect transistors

Semiconducting nanotubes can work as transistors. The tube can be “turned on” – i.e. made to conduct – by applying a negative bias to the gate, and “turned off” with a positive bias (Fig. 3a). A negative bias induces holes on the tube and makes it conductive. Positive biases, on the other hand, depletes the holes and decrease the conductance. Indeed, the resistance of the “off” state can be more than a million times greater than the “on” state. This behaviour is

analogous to that of a p-type metal-oxide-silicon field effect transistor (MOSFET), except that the nanotube replaces silicon as the material that hosts the charge carriers.

The reason why carbon nanotube appears as p-type instead of intrinsic semiconductor is that the metal electrodes “dope” the tube to be p-type. In other words, they remove electrons from the tube, leaving the remaining mobile holes responsible for conduction. Indeed, recent experiments show that changing a tube’s chemical environment can change the level of doping, significantly changing the voltage at which the device is turned on [15]. More dramatically, tubes can even be doped n-type by exposing the tube to elements such as potassium that donates electrons to the tube.

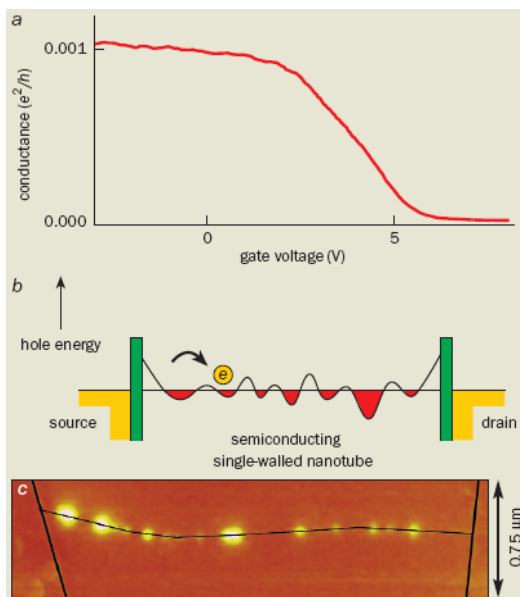


**Fig. 5:**

(a) The conductance of a semiconducting carbon nanotubes as a function of gate voltage.

(b) The potential profiles seen by these holes due to disorder in the structure of the nanotube and imperfect contacts between the electrodes and the tube.

(c) The tip of a scanning probe microscope can be used to map the barriers to conduction [14]



The semiconducting device of the type shown in Fig. 5 is, in many ways, truly remarkable. First, it is only one nanometre wide. While much work has been done to create ultra-small semiconducting devices from bulk semiconductors, such devices have always been plagued by “surface states” --- electronic states that arise when a three-dimensional crystal is interrupted by a surface. These surface states generally degrade the operating properties of the device, and controlling them is one of the key technological challenges to device miniaturization. Nanotubes solve the surface-state problem in an elegant fashion. First, they are inherently 2D materials, so the problem of a 3D lattice meeting a surface does not exist. Second, they avoid the problem of edges because of the seamlessly wrapped graphene sheet.

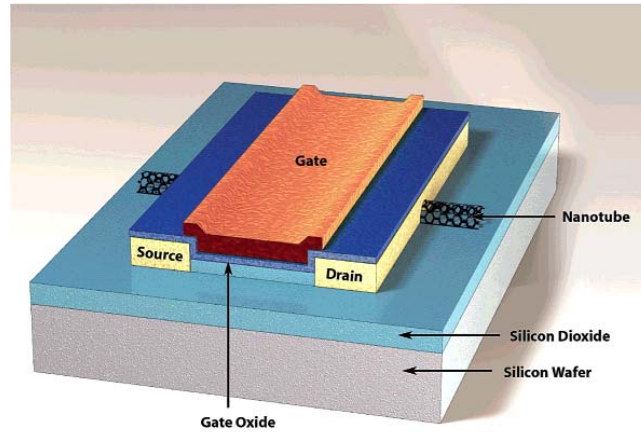


**Fig. 6:**  
Schematic representation of a top-gated CNTFET.

Carbon nanotube field effect transistor (CNTFET) is shown in Fig. 6. These tiny devices will probably just be the first in a host of new semiconducting-device structures based on carbon nanotubes. Other devices, such as nanotube p–n junction diodes and bipolar transistors, have been discussed theoretically and are likely to be realized soon.

#### 4. Metallic CNTs as 1D Metal

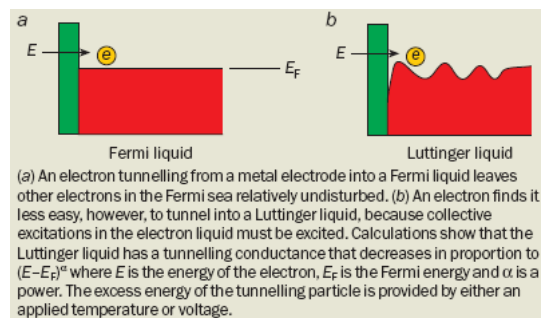


**Fig. 7:**  
Comparison between Fermi liquid and Luttinger liquid

In dramatic contrast to semiconducting nanotubes, the conductance of some other nanotubes near room temperature is not noticeably affected by the addition of a few carriers. This behaviour is typical of metals, which have a large number of carriers and have conducting properties that are not significantly affected by the addition of a few more carriers. The conductance of these metallic nanotubes is also much larger than that of the semiconducting-

nanotube devices, as expected. Indeed, a number of groups have made tubes with conductances that are between 25% and 50% of the value of  $4e^2/h$  that has been predicted for perfectly conducting ballistic nanotubes. This result indicates that electrons can travel for distances of several microns down a tube before they are scattered. Several measurements support this conclusion [16]. These measurements also show that the contact resistance between the tube and the electrodes can be substantial, just as it is with semiconducting tubes.

Further evidence for the near-perfect nature of these tubes comes from the way they behave at low temperatures. The conductance is observed to oscillate as a function of gate voltage. These “Coulomb oscillations” occur each time an additional electron is added to the nanotube. In essence, the tube acts like a long box for electrons, often called a “quantum dot” [17]. The electronic and magnetic properties of these nanotube quantum dots reveal a great deal about the behaviour of electrons in nanotubes. For example, the fact that the oscillations are quite regular and periodic indicates that the electronic states are extended along the entire length of the tube. If, however, there was significant scattering in the tube, the states would become localized and the Coulomb oscillations would be less regular. Nanotube quantum dots that are as long as 10  $\mu\text{m}$  have been found to exhibit these well-ordered oscillations, again indicating that the mean free path can be very long.

The experiments described above indicate that electrons can travel for long distances in nanotubes without being backscattered. This is in striking contrast to the behaviour observed in traditional metals like copper, in which scattering lengths from lattice vibrations are typically only several nanometres at room temperature. The main reason for this remarkable difference is that an electron in a 1-D system (like a nanotube) can only scatter by completely reversing its direction, whereas electrons in a 2D or 3D material can scatter by simply changing direction through a tiny angle. Phonons do not have enough momentum to reverse the direction of a speeding electron in a 1-D nanotube. They therefore do not influence its conductance, at least not at low voltages. Fig. 7 shows this contrast between normal metal and 1D metallic nanotube.

Experiments clearly demonstrate that interacting 1-D metals behave very differently to 2-D and 3-D metals. This is perhaps not so surprising – to use a traffic analogy, car-car interactions are much more important on a one-lane highway than they are in a 2-D parking lot, where a car can move more-or-less independently of the other cars. What is surprising, however, is how long it took before these predictions were tested in detail. While probes, successive measurements of other systems had shown evidence for Luttinger behaviour, nanotubes represent perhaps the clearest and most straightforward realization of Luttinger-liquid physics to date.

## **5. Outlook: Novel Devices composed of 1D-Geometric Electronics**

New devices can be created by the intersection of two nanotubes, such as a metallic tube crossing over a semiconducting tube (Fig. 8). The metallic tube locally depletes the holes in the underlying p-type semiconducting tube. This means that an electron traversing the semiconducting tube must overcome the barrier created by this metal tube. Biasing one end of the semiconducting tube relative to the metal tube leads to rectifying behaviour. In other words, the barrier is overcome in one bias direction, but not in the other. This structure is just one of many possibilities for nanotube devices waiting to be explored.

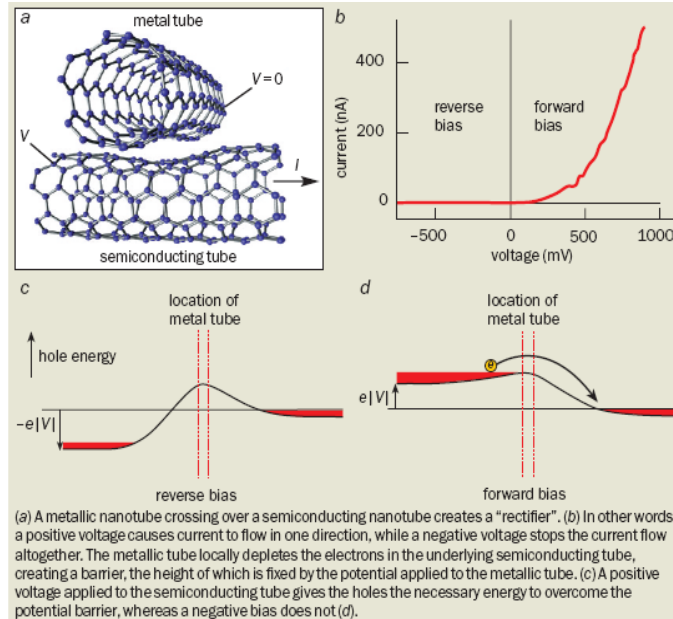


**Fig. 8:** Illustrations for a novel electronic device "rectifier" consists of a semiconducting and a metallic carbon nanotube. [17]

Many commercial applications have been proposed, from molecular electronic devices to sensors. Whether these can be realized is more difficult to assess [18]. If these real-world applications of nanotubes are achieved, we still need to find out ways of successfully integrate them into existing microelectronic systems. But if we manage to develop the technology to fabricate nanotubes of a particular type, length and diameter in a controlled fashion – and to incorporate the tubes into lithographic circuits at particular places with efficiencies approaching 100%, then only the sky is the limit. While this is a challenging goal, there appears to be no fundamental barriers for achieving it. A proper marriage of physics, chemistry and electrical engineering may be up to the task. Electronics may start to follow the way of biology and use the carbon atom as its backbone.

#### References:

- [1] S. G. Louie, *Top. Appl. Phys.* **80**, 113 (2001).
- [2] J. W. G. Wildoer, L. C. Venema, A. G. Rinzler, R. E. Smalley, C. Dekker, *Nature* **391**, 59 (1998).
- [3] A. Thess *et al.*, *Science* **273**, 483 (1996).
- [4] R. H. Baughman *et al.*, *Science* **297**, 787 (2002).
- [5] M. P. Anantram and F. Leonard, *Rep. Pro. Phys.* **69**, 507 (2006).
- [6] G. S. Painter and D. E. Ellis, *Phys. Rev. B* **1**, 4747 (1970)
- [7] R. Saito, G. Dresselhaus and M. S. Dresselhaus, *Physical Properties of Carbon Nanotubes*, Imperial College Press (1998)
- [8] R. A. Jishi, *et al.*, *J. Phys. Soc. Jpn.* **63**, 2252 (1994)
- [9] C. T. White, D. H. Robertson and J. W. Mintmire, *Phys. Rev. B* **47**, 5485 (1993).
- [10] C. T. White and J. W. Mintmire, *J. Phys. Chem. B* **109**, 52 (2005).
- [11] J. W. Mintmire and C. T. White, *Phys. Rev. Lett.* **81**, 2506 (1998).
- [12] I. Cabria, J. W. Mintmire and C. T. White, *Phys. Rev. B* **67**, 121406 (2003).
- [13] X. Blase *et al.*, *Phys. Rev. Lett.* **72**, 1878 (1994).
- [14] P. L. McEuen, *Physics World* **13**, 31 (2000).
- [15] C. Zhou, J. Kong, E. Yenilmez and H. Dai, *Science* **290**, 1552 (2000)
- [16] M. Bockrath *et al.*, *Phys. Rev. B* **61**, R10606 (2000)
- [17] L. Kouwenhoven and C. Marcus, *Physics World* **11**, 35 (1998).
- [18] W. H. A de, R. Martel, *Physics World* **13**, 49 (2000).